On the microstructure of thin films grown by an isotropically directed deposition flux

R. Alvarez, P. Romero-Gomez, J. Gil-Rostra, J. Cotrino, F. Yubero, A. Palmero, and A. R. Gonzalez-Elipe

Citation: Journal of Applied Physics **108**, 064316 (2010); doi: 10.1063/1.3483242
View online: http://dx.doi.org/10.1063/1.3483242
View Table of Contents: http://scitation.aip.org/content/aip/journal/jap/108/6?ver=pdfcov
Published by the AIP Publishing

On the microstructure of thin films grown by an isotropically directed deposition flux

R. Alvarez,[1,a)] P. Romero-Gomez,[1] J. Gil-Rostra,[1] J. Cotrino,[1,2] F. Yubero,[1] A. Palmero,[1] and A. R. Gonzalez-Elipe[1]
[1]*Instituto de Ciencia de Materiales de Sevilla, CSIC–Universidad de Sevilla, Av. Américo Vespucio 49, 41092 Sevilla, Spain*
[2]*Departamento de Física Atómica, Molecular y Nuclear, Universidad de Sevilla, Avda. Reina Mercedes, s/n, 41012 Sevilla, Spain*

(Received 26 April 2010; accepted 27 July 2010; published online 22 September 2010)

The influence of isotropically directed deposition flux on the formation of the thin film microstructure at low temperatures is studied. For this purpose we have deposited TiO_2 thin films by two different deposition techniques: reactive magnetron sputtering, in two different experimental configurations, and plasma enhanced chemical vapor deposition. The obtained results indicate that films grown under conditions where deposition particles do not possess a clear directionality, and in the absence of a relevant plasma/film interaction, present similar refractive indices no matter the deposition technique employed. The film morphology is also similar and consists of a granular surface topography and a columnarlike structure in the bulk whose diameter increases almost linearly with the film thickness. The deposition has been simulated by means of a Monte Carlo model, taking into account the main processes during growth. The agreement between simulations and experimental results indicates that the obtained microstructures are a consequence of the incorporation of low-energy, isotropically directed, deposition particles. © *2010 American Institute of Physics*. [doi:10.1063/1.3483242]

I. INTRODUCTION

Plasma assisted deposition techniques are widely used for the growth of thin films with different microstructures and properties.[1–3] In general, film growth involves the incorporation of species injected or formed in the plasma phase onto the growing film surface, as well as the impingement of plasma species and photons in a far from equilibrium situation.[4] Diverse experiments as well as computational models point out the importance of several fundamental mechanisms on the formation and evolution of the film microstructure during growth, e.g., thermally activated surface processes,[5] impingement of charged species on the film surface,[6] short and long range interactions,[7] potential barriers,[8] desorption,[9] etc. On the other hand, actual experimental parameters during film deposition hardly permit an accurate control of these processes, so the coupling between experimental conditions and the deposited thin film microstructure is usually based on empirical relations rather than on predictive models (see for instance Refs. 10–12). Consequently, the study and analysis of the role of these fundamental processes, as well as their experimental control, represent an important area of research for the synthesis of tailored thin films.

There are few theoretical models in the literature that analyze the growth of films deposited by plasma-assisted techniques (see for instance Ref. 13, and references therein). Due to the amount of particles involved and the typical times required for the film growth, the use of first principles or molecular dynamics approaches is not recommended due to unaffordable computational costs. In this way, Monte Carlo (MC) models represent an alternative theoretical tool to study the film deposition, whereby the deposition particles may experience different interactions that are introduced *ad hoc* into the model. However, the extreme difficulty in describing the plasma/surface interaction, strongly coupled to processes in the plasma bulk and sheath, as well as the necessity of including the film surface chemistry, have not yet permitted the development of general models. This means that MC models can only be used in particular situations where certain mechanisms are known to be responsible for the film growth, such as geometric mechanisms (surface shadowing, different angular distribution of the arriving particles), adherence mechanisms (presence or not of overhangs, bouncing of the arriving particles), thermal related mechanisms (surface diffusion, desorption) etc.[13–16]

One of the key factors determining the film surface morphology is the angular distribution of the particles arriving at the substrate which, in connection with the surface shadowing mechanism, was studied by us in a previous publication.[14] There, we found a strong correlation between the directionality of the deposition particles and the critical exponents which, stemming from a dynamic scaling approach,[13] describe the evolution of the surface topography. This approach was also sustained in Ref. 15 where we found a clear relation between particle directionality and the size of the mounds formed on the surface of pulsed laser deposited ZrO_2 thin films. In Ref. 15 we also studied the competition between surface shadowing and thermally activated surface diffusion, obtaining that, at high film temperatures and/or low deposition rates, the influence of surface shadowing, and through it of particle directionality, becomes less important

a)Electronic mail: rafael.alvarez@icmse.csic.es.

when defining the surface morphology. This has also been reported in the literature by different authors which take into account other processes, such as re-emission of high energy deposition particles, desorption mechanism at high temperatures, potential barriers, etc. (see Refs. 5–9, 14, and 16, and references therein).

A well known deposition technique where particle directionality plays an important role is the so-called reactive magnetron sputtering (MS) deposition, which is one of the most popular in the industry and in research centers due to its reproducibility, versatility, and high deposition rates.[17] Here, a plasma, most likely argon, is maintained by injecting electromagnetic power through a solid material, the so-called cathode or target, making positive ions from the plasma impinge on it and sputter some atoms with kinetic energies in the order of few tens of electron volt.[18] In addition, a small amount of a reactive gas is injected into the plasma, which produces reactive species that reach the surface, thus controlling the film composition. Sputtered species possess high energy (typically their mean kinetic energy is in the order of 10–20 eV) and a well defined directionality when leaving the cathode (usually they follow a very narrow angular distribution function of the type $\cos^2 \psi$, being ψ the emission angle with respect to the normal of the cathode[18]). Nevertheless, scattering processes in the plasma phase may alter both, the kinetic energy of the sputtered particle and its directionality.[19] In this way, when the mean free path of the sputtered particles is larger than the target-film distance (low plasma density conditions), sputtered atoms arrive at the growing surface with almost their original energy and momentum (ballistic flow). Conversely, when this mean free path is smaller than the distance target-film (high plasma density conditions), sputtered particles may experience several collisions and lose their original directionality and kinetic energy. In a limit situation, these sputtered particles may end up in thermal equilibrium with the neutral particles of the plasma, thus following an isotropic velocity distribution function when arriving at the film surface (isotropic flow).[20] In addition to MS depositions, isotropically directed particles are involved in the film growth when using other deposition techniques, such as plasma enhanced chemical vapor deposition (PECVD), for instance. In this technique, most plasma particles approximately follow an isotropic velocity distribution function when arriving at the film surface, except those possessing electrical charge, which are accelerated by the plasma sheath.[13]

In this paper we theoretically and experimentally study the microstructure of films grown by the incorporation of low-energy, isotropically directed, deposition particles in the absence of (or under a weak) plasma/surface interaction. As we will see, films grown under these conditions develop a characteristic microstructure, independently of the particular deposition technique employed. For this purpose we have deposited thin films through the PECVD and MS deposition methods in two different experimental configurations. From the comparison between the obtained microstructures and with the help of a MC model we have studied and discussed the features of the resulting films. We would like to emphasize that we focus on the characterization of the film microstructure, i.e., its bulk, and not on the film surface morphology. The bulk of the film determines in a great extent its optical, electrical, or mechanical properties, so its characterization is of relevance for the study of thin films and their applications. Finally, although our results have a general character, the experiments have been carried out by depositing amorphous TiO_2 thin films as a test material. This choice is supported by the wide use of this material for a large number of applications[21] where a tight correlation usually exists between microstructure and functional properties.[22]

This paper is organized as follows: in Sec. II we describe the experimental setup, whereas in Sec. III we explain the MC model developed to explain the depositions. In Sec. IV we describe and discuss the results, and finally in Sec. V we summarize the conclusions.

II. EXPERIMENTAL SETUP

Amorphous TiO_2 thin films were grown on silicon substrates by means of the reactive MS deposition technique. An unbalanced cathode with a 2 in. diameter Ti target, powered by a MacCo pulsed dc power supply (80 kHz pulse frequency and 40% duty cycle) was used as a source of Ti atoms. A grounded substrate holder was placed 7 cm apart from the target in front of the center of the cathode, and parallel to it. Argon and oxygen flows were set up at 10 SCCM and 1.3 SCCM, respectively (SCCM denotes cubic centimeter per minute at STP) resulting into a total deposition pressure of 0.5 Pa. The electromagnetic power was set to 300 W, with a net current at the cathode of 0.6 A. Amorphous TiO_2 thin films were deposited in two different configurations: the first one, which we call *direct deposition* (d-MS), corresponds to the typical MS configuration where the film is placed on the side of the holder facing the cathode. The second configuration, which we call *inverse deposition* (i-MS), according to the terminology used in pulsed laser depositions,[23] corresponds to a substrate attached to the back side of the holder, not facing the cathode (see Fig. 1). Film temperature, monitored during the deposition, was always below 320 K. Deposition rates of 4 nm/min and 1.3 nm/min were determined for d-MS and i-MS depositions, respectively.

TiO_2 thin films were also grown on a silicon substrate by PECVD according to a previously described experimental protocol.[12] The technique uses oxygen plasma sustained by a microwave source and a deposition system which consists of a source of volatile precursor (i.e., titanium tetrakis isopropoxide) in a downstream configuration, separated from the plasma by a grounded grid to avoid the microwave heating of the substrates and to diminish the arrival of charged species at the deposition region. The source was operated with a power of 400 W and an oxygen pressure of 0.8 Pa. Film temperature was monitored during the deposition and found to be room temperature. A deposition rate of 2 nm/min was obtained under these experimental conditions.

The refractive index of the films, n_r, was measured in transmission mode by ultraviolet-visible absorption spectroscopy technique for films grown on quartz plates. Similar values were obtained for thin films grown on a silicon wafer

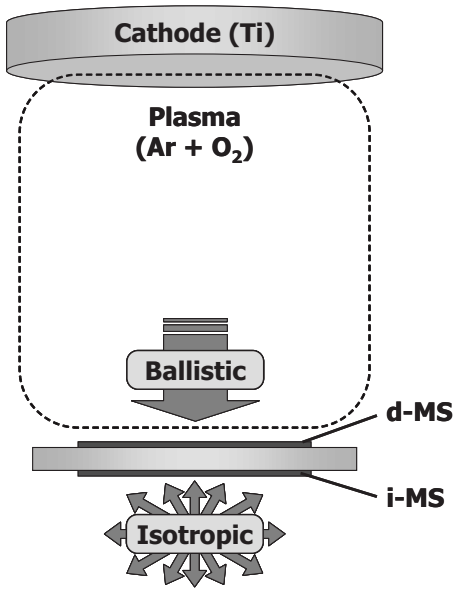

FIG. 1. Scheme of the MS deposition setup in the direct (d-MS) and inverse (i-MS) configurations. At low plasma densities, the contribution of ballistic particles on the growth of the film in the d-MS configuration is dominant. Conversely, in the i-MS configuration only the isotropic flow contributes to the film growth.

measured in reflection mode. Field emission scanning electron microscopy (FESEM) images of the films were obtained by cleaving the silicon substrates with the deposited films (i.e., cross-section views) or by looking directly to their surface (i.e., normal views).

III. THEORETICAL MODEL

In our model we consider the deposition of effective particles on a two-dimensional substrate that defines the x-y plane of coordinates, whereas the z axis is defined by the direction perpendicular to the substrate. The three dimensional space is divided into a $N_L \times N_L \times N_H$ cubic grid, each cell representing a spatial volume of Δ^3, whose value is 1 if it contains a deposited effective particle and 0 otherwise. Each effective particle moves toward the substrate from an initial random position above the film and follows the direction defined by the spherical angles θ and φ, where $\theta \in [0, \pi/2)$ is the polar angle of incidence ($\theta=0$ is the direction normal to the substrate) and $\varphi \in [0, 2\pi)$ is the azimuthal angle. The movement of the particle continues, assuming periodic boundary conditions, until it hits the surface where it sticks (see Fig. 2). The angles θ and φ are randomly calculated for each deposition particle by defining an incident angle distribution function per unit time and unit surface, $I(\Omega)$, with $d\Omega = \sin\theta d\theta d\varphi$ the differential solid angle. When the deposition particles are isotropically directed in the plasma phase, this function takes the form $dI(\Omega) = d\Omega \int_0^{+\infty} d\mathrm{v} \mathrm{v}^2 f(\mathrm{v}) \vec{\mathrm{v}} \cdot \vec{s} \propto \cos\theta d\Omega$, where $\vec{\mathrm{v}}$ is the velocity vector, v its modulus, $f(\mathrm{v})$ the velocity distribution function of the deposition particles in the gas phase (note that it only depends on v because it is isotropic), and $\vec{s}$ a unit vector perpendicular to the deposition surface.[13]

From a physical point of view, each particle in the model accounts for a Ti species that, after being deposited, instantaneously turns into a TiO_2 effective block, occupying a cubic volume Δ^3. This imposes an important constrain in our model, as the structure of amorphous TiO_2 is not cubic but mainly made of deformed octahedra, with average distances between Ti atoms between 3 and 4 Å.[24] Conversely, by knowing the typical distances in the material we can estimate the value of Δ: we approximate Δ as the actual average distance between two Ti atoms in the amorphous network, i.e., $\Delta \sim 3.5$ Å. In the MC model we have not introduced neither surface diffusion nor desorption mechanisms, due to the low temperature of the film during growth. Moreover, in agreement with in Ref. 25, the low-energy of the deposition particles made us neglect any re-emission of deposition particles. Finally, no Schwoebel potential barrier has been considered, as there are not well-defined atomic steps on an amorphous surface.[26]

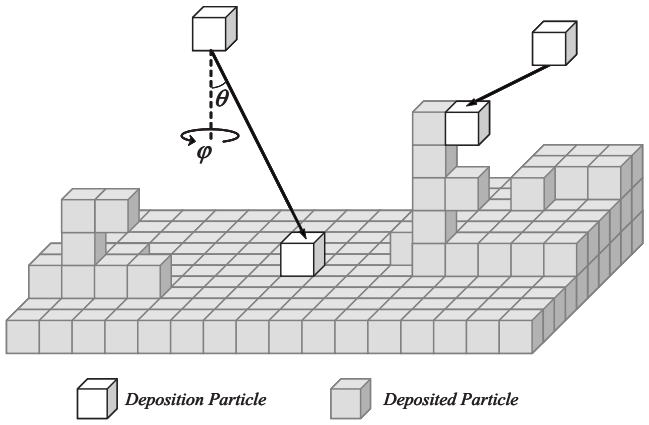

FIG. 2. Scheme of the processes taken into account in the MC model.

Simulations have been carried out for increasing values of N_L (up to $N_L=2000$) to avoid finite size effects on the solutions. Particles were accumulated until the maximum height of the simulated film was close to that of the experimental values (assuming $\Delta \sim 3.5$ Å).

IV. RESULTS AND DISCUSSION

In Figs. 3(a) and 4(a) we show, respectively, the cross-sectional and top view FESEM images of a film deposited in the d-MS configuration. It is apparent in these images that the film (about 230 nm thick) grows compact, developing an almost flat surface topography with some mounds. In Figs. 3(b) and 4(b) we show the FESEM images of, respectively, the cross-sectional and top views of the film deposited by i-MS: film thickness is about 110 nm, and, in this case, a very different microstructure is grown. Figure 4(b) shows a granular surface topography, whereas Fig. 3(b) depicts nonregular columnlike structures whose diameters increase as we move apart from the substrate. By using standard techniques of image treatment, such as those employed in granulometry, we have been able to determine the average width of these structures at a given height. These results are shown in Fig. 5, where it can be seen that the width of the columnlike structures seems to increase almost linearly as we move apart from the substrate. It is also noticeable in this figure the

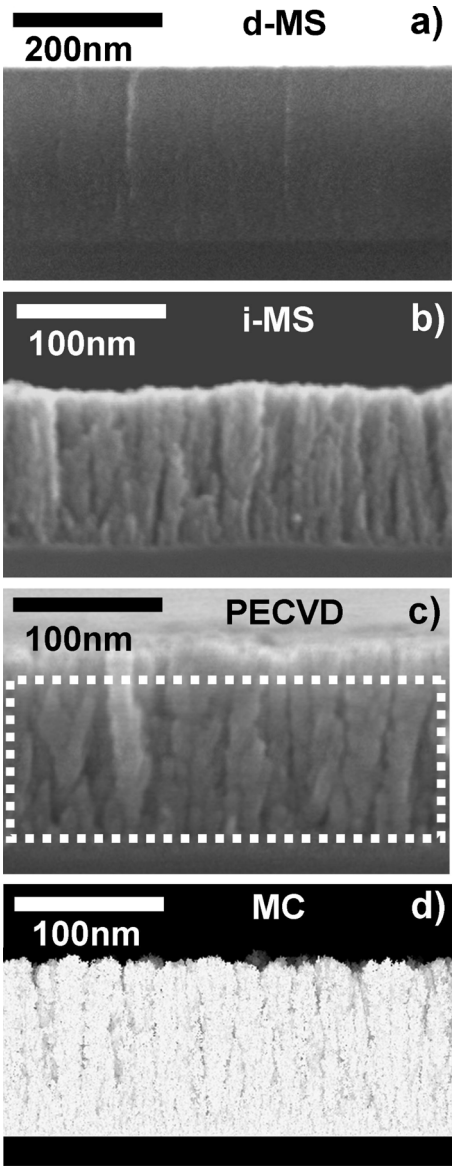

FIG. 3. Cross-sectional images of films obtained by (a) the d-MS experimental configuration, (b) the i-MS experimental configuration, (c) the PECVD technique, and (d) the MC model. FESEM technique was used for (a), (b), and (c).

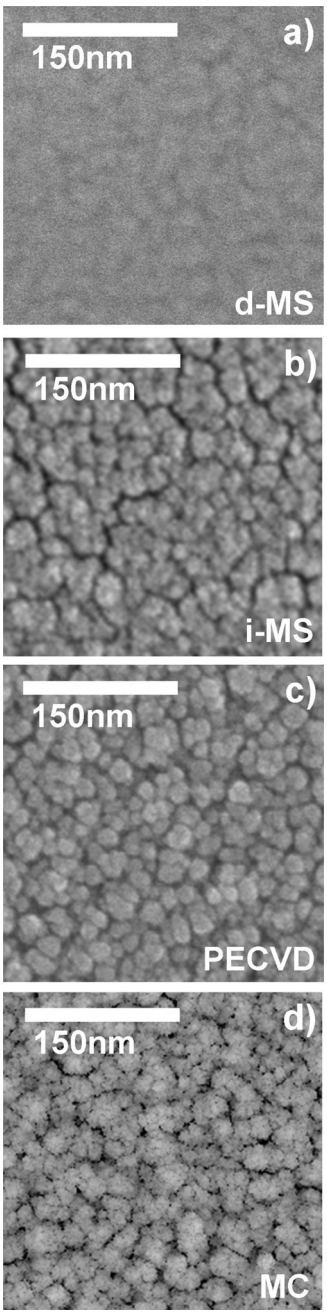

FIG. 4. Top view images of films obtained by (a) the d-MS experimental configuration, (b) the i-MS experimental configuration, (c) the PECVD technique, and (d) the MC model. FESEM technique was used for (a), (b), and (c).

fairly good agreement between the width of the motives for the maximum height and the average diameter of the surface mounds shown in Fig. 4(b).

It is well established in the literature that the growth of MS deposited metal-oxide thin films involves the incorporation of sputtered atoms, typically with a sticking probability close to 1, whose free bonds quickly saturate with oxygen species arriving from the gas/plasma phase (see for instance Ref. 27). In this way, the microstructural differences found between d- and i-MS deposited films can be attributed to the different directionality and energy of the titanium atoms, as well as to the interaction with the plasma: in Ref. 20 we derived the ratio of the sputtering rate, Φ_0, and the deposition rate, r, as a function of the deposition conditions: when the temperature of the heavy particles in the plasma can be taken as constant in the discharge, this relation yields

$$\frac{r}{\Phi_0} = \frac{\lambda_T}{L}\left[1 - \exp\left(-\frac{L}{\lambda_T}\right)\right], \tag{1}$$

where L is the distance between the target and the film, and λ_T the so-called thermalization mean free path. The fundamental assumption made in this model is that a ballistic sputtered particle is effectively thermalized in one collision with a neutral background gas particle. Since this assumption is not realistic for sputtered atoms heavier than the sputtering gas atoms, we introduced an effective elastic scattering cross-section, σ_T, which takes into account that more than one collision might be necessary to transfer an atom from the ballistic to the isotropic flow. Thus $\lambda_T=(N\sigma_T)^{-1}$, where N is

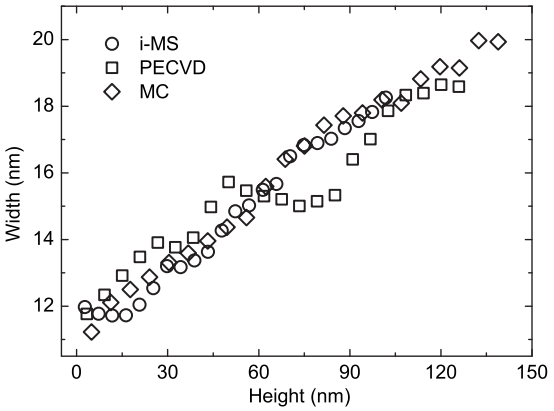

FIG. 5. Average width of the columnlike structures in the bulk of the films deposited by i-MS and PECVD, together with that of the MC simulated thin film.

the density of heavy particles in the plasma. Despite the fact that this is a very simplistic description, Eq. (1) has proven adequate to describe the deposition of many films, finding the relation $\sigma_T \approx \sigma_g/\nu$, with ν being the average number of collisions required for the thermalization of a sputtered particle and σ_g the geometrical cross-section for an elastic scattering of a sputtered particle on a plasma heavy particle.[28] In order to evaluate the proportion of ballistic and isotropic flows toward the film in our d-MS configuration, we have used data appearing in Ref. 28: the geometrical cross-section for an elastic scattering of a Ti atom on an Ar atom is $\sigma_g = 5 \times 10^{-20}$ m^2, whereas the thermalization cross-section is $\sigma_T \sim 2 \times 10^{-20}$ m^2. The relative ballistic contribution to direct growth is estimated as $\Phi_0 \exp(-L/\lambda_T)/r$, which under our experimental conditions, gives that approximately 90% of the titanium species reach the holder with high energy and well defined directionality, whereas about 10% of them were previously thermalized in the plasma phase.

When the deposition is performed using the i-MS configuration of the experimental setup, we can assume that no ballistic particles arrive at the film surface. We neglect, therefore, the ballistic Ti atoms that have been backscattered by other plasma particles and reach the back side of the holder with clear directionality. This has been done because the probability that these particles reach the film surface is very low (indeed, few collisions are required to thermalize the titanium atoms in the argon plasma, $\nu \sim 2.5$ in this case[28]). Moreover, we consider that the influence of ions, high energy photons or species from the plasma in metastable excited states, present in the d-MS configuration, are negligible in the i-MS deposition. This assumption is supported by the experimental observation that no plasma glow during deposition develops at the back side of the substrate holder. In this way, by studying films deposited in the i-MS configuration we can study the growth of the film when low-energy, isotropically directed deposition particles incorporate to the film in the absence of plasma/surface interaction.

Amorphous TiO_2 thin films were deposited by PECVD according to the procedure described in Sec. II. In Ref. 12 we showed that, in this case, the film grows due to the incorporation of Ti species from the plasma phase that, after landing on the film surface, react with plasma species forming O–Ti–O bonds in the material. Moreover, due to the characteristics of the deposition technique and the experimental configuration utilized, the Ti species arrive at the film surface with an isotropic velocity distribution function, remaining on the surface with a low mobility due to the low film temperature.[29] The remote plasma configuration as well as the presence of the grounded grid between the plasma and the substrate holder makes us neglect the influence of ions on the film growth. In Figs. 3(c) and 4(c) we show FESEM images of, respectively, the cross-sectional and top views of a TiO_2 thin film deposited by PECVD, which are similar to those in Ref. 12. At a glance, it is clear that these images present many common features with those obtained for i-MS deposited TiO_2 thin films [Figs. 3(b) and 4(b)], being their microstructure and surface morphology very alike. In Fig. 3(c), the columnlike structures grow perpendicular to the substrate and increase in width as the film grows. To stress this correspondence, we have also depicted the width of these structures as a function of height in Fig. 5, finding a good match with that of the i-MS deposited thin film. Regarding the width at the maximum height in Fig. 5, we find that the size of the surface mounds correlates well for similar heights, although their shape is more rounded than those in Fig. 4(b).

The measured refractive index for the d-MS deposited thin film is $n_r = 2.40$, which agrees with typical values for TiO_2 thin films at room temperature deposited in this configuration.[30] On the other hand, the measured refractive index of the i-MS deposited thin film was $n_r = 1.92$, which agrees quite well with the measured index of the films grown by the PECVD technique at low temperatures ($n_r \sim 1.93$).[30] The strong connection between the value of the refractive index and the particular microstructure of a given material has been extensively studied in the literature. To a first approximation, provided that the materials do not present quite different pore size distributions and connectivity, the refractive index and relative pore volume are two related properties (see for instance Ref. 22). Therefore, the good correspondence between the values of n_r obtained for the TiO_2 films deposited by i-MS and PECVD suggests possible microstructural similarities. The film deposited in the d-MS configuration, on the other hand, possess a higher refractive index indicating a higher degree of compactness and a different microstructure.

We have, therefore, shown that not only the refractive indexes in the PECVD and i-MS TiO_2 deposited thin films are similar but also the geometrical motives in the bulk, and their size. This similarity could be understood by analyzing both depositions methods: a common feature in both cases is that the film growth is governed by the deposition of low-energy Ti species from the plasma phase that arrive at the growing surface with an isotropic velocity distribution function. Moreover, although the surface processes experienced by these titanium species are very different, they eventually become fully oxidized, being their incorporation to the material controlled by a similar shadowing mechanism. In order to account for the abovementioned deposition mechanisms, we have developed the MC model described in Sec. III: in Figs. 3(d) and 4(d) we depict the simulated cross-sectional

and top views of the films, respectively. In these figures we can see that the simulated microstructure agrees fairly well with the experimental ones [shown in Figs. 3(b), 3(c), 4(b), and 4(c)]: they develop a similar columnlike microstructure, with increasing diameters as we move apart from the substrate, as well as a granular surface morphology with motives of similar relative size. In Fig. 5 we have also depicted the average diameters of the columns of the simulated film as a function of height, showing a good agreement with the equivalent representation made for the films deposited by i-MS and PECVD. Regarding the width of the calculated motives for the maximum height (i.e., the average size of the calculated surface grains) we also conclude that our model reproduces well surface features of both films, shown in Figs. 3(b), 3(c), 4(b), and 4(c), and explains why the microstructures of the films deposited by the i-MS and the PECVD techniques are similar. Nevertheless, the MC model does not explain the existing shape discrepancies between surface grains in Figs. 4(b) and 4(c), which we attribute to the different surface chemistry involved in PECVD and i-MS depositions, which has not been taken into account in our model. Our results also illustrate the importance of analyzing the bulk features, and not only the surface morphology, when studying the growth of thin films and their properties.

The complexity of the several possible mechanisms involved in the d-MS deposition of thin films makes the description of the film growth rather difficult in this case. For instance, the relatively high kinetic energy of a ballistic particle when arriving at the film surface may induce the so-called re-emission process, implying that the deposition particle may "bounce off" on the film surface until it sticks to the material or it is desorbed, generating a net downhill current of deposition particles toward the substrate.[31] Furthermore, the impingement of ions, photons, and other species from the plasma on the film surface produce diverse effects, such as the increase in the compactness of the material and the rise of the film temperature, and thus higher efficiency of the thermally activated surface diffusion mechanisms. The development of a MC model describing the film growth under these conditions is far from the scope of this paper. Nevertheless, some qualitative conclusions can be achieved regarding the higher refractive index for the d-MS thin film in comparison with those obtained for PECVD and i-MS thin films, as well as by comparing Figs. 3(a) and 3(b): d-MS deposited thin films are more compact and without clear motives on the bulk, features that agree with the deposition of high energy particles in a strong plasma/surface interaction environment (most likely under a relevant ion impingement on the film surface during growth). Nevertheless these obtained features for d-MS depositions depend on the plasma conditions and, therefore, they do not represent a general result within the plasma-assisted thin film deposition research.

V. CONCLUSIONS

In this paper we have studied the growth and microstructure of films deposited by the MS technique in two different configurations, and by the PECVD technique at low temperature in a remote configuration. Thin films deposited by MS when the substrate holder was facing the cathode possess a compact bulk structure with a granular surface topography and a relatively high refractive index. Meanwhile, films deposited when the substrate holder was not facing the cathode develop a microstructure similar to that of TiO_2 thin films deposited by the PECVD technique: they possess a clear columnlike structure, granular surface morphology and similar refractive index. In addition, we have developed a MC simulation of the film growth that takes into account the deposition and shadowing of particles that follow an isotropic velocity distribution function. This model explains the main microstructural features of the films deposited by PECVD and MS when the film is not facing the cathode, indicating the importance of isotropic deposition particles in the formation of the microstructure in plasma-assisted deposition of thin films. Our results are, therefore, relevant to understand the role of the different plasma/gas species in the formation of the film microstructure.

ACKNOWLEDGMENTS

R. Álvarez acknowledges the JAE program of the Spanish Council of Research (CSIC). Financial support from the Spanish Ministry of Innovation (Project No. MAT 2007-65764, CONSOLIDER INGENIO 2010-CSD2008-00023 and PIE 200960I132) and the Junta de Andalucía (Project Nos. TEP2275 and P07-FQM-03298) is acknowledged.

[1] S. V. Vladimirov and K. Ostrikov, Phys. Rep. **393**, 175 (2004).
[2] A. E. Rider, I. Levchenko, and K. Ostrikov, J. Appl. Phys. **101**, 044306 (2007).
[3] M. Capitelli, R. Celiberto, F. Esposito, and A. Laricchiuta, Plasma Processes Polym. **6**, 279 (2009).
[4] E. Tam, I. Levchenko, K. Ostrikov, M. Keidar, and S. Xu, Phys. Plasmas **14**, 033503 (2007).
[5] Y. G. Yang, R. A. Johnson, and H. N. G. Wadley, Acta Mater. **45**, 1455 (1997).
[6] S. Mráz and J. M. Schneider, J. Appl. Phys. **100**, 023503 (2006).
[7] J. Yu and J. G. Amar, Phys. Rev. Lett. **89**, 286103 (2002).
[8] J. G. Amar and F. Family, Phys. Rev. B **54**, 14742 (1996).
[9] S. Schinzer, M. Sokolowski, M. Biehl, and W. Kinzel, Phys. Rev. B **60**, 2893 (1999).
[10] S. S. Huang and J. S. Chen, J. Mater. Sci.: Mater. Electron. **13**, 77 (2002).
[11] M. J. Aziz, Appl. Phys. A: Mater. Sci. Process. **93**, 579 (2008).
[12] A. Borrás, J. Cotrino, and A. R. González-Elipe, J. Electrochem. Soc. **154**, P152 (2007).
[13] M. Pelliccione and T.-M. Lu, *Evolution of Thin Film Morphology* (Springer-Verlag, Berlin, 2008).
[14] A. Yanguas-Gil, J. Cotrino, A. Barranco, and A. R. Gonzalez-Elipe, Phys. Rev. Lett. **96**, 236101 (2006).
[15] R. Álvarez, A. Palmero, L. O. Prieto-López, F. Yubero, J. Cotrino, W. de la Cruz, H. Rudolph, F. H. P. M. Habraken, and A. R. Gonzalez-Elipe, J. Appl. Phys. **107**, 054311 (2010).
[16] M. Pelliccione, T. Karabacak, C. Gaire, G.-C. Wang, and T.-M. Lu, Phys. Rev. B **74**, 125420 (2006).
[17] J. M. Schneider, S. Rohde, W. D. Sproul, and A. Matthews, J. Phys. D **33**, 201 (2000).
[18] J. A. Thornton and J. E. Greene, in *Handbook of Deposition Technologies for Films and Coatings*, 2nd ed., edited by R. F. Bunshah (Noyes, New Jersey, 1994), p. 274.
[19] A. Palmero, H. Rudolph, and F. H. P. M. Habraken, Appl. Phys. Lett. **87**, 071501 (2005).
[20] A. Palmero, H. Rudolph, and F. H. P. M. Habraken, Appl. Phys. Lett. **89**, 211501 (2006).
[21] O. Carp, C. L. Huisman, and A. Reller, Prog. Solid State Chem. **32**, 33 (2004).
[22] A. Borras, J. R. Sanchez-Valencia, J. Garrido-Molinero, A. Barranco, and

A. R. Gonzalez-Elipe, Microporous Mesoporous Mater. **118**, 314 (2009).
[23]T. Szörényi, B. Hopp, and Z. Geretovszky, Appl. Phys. A: Mater. Sci. Process. **79**, 1207 (2004).
[24]V. Van Hoang, Phys. Status Solidi B **244**, 1280 (2007).
[25]J. T. Drotar, Y.-P. Zhao, T.-M. Lu, and G.-C. Wang, Phys. Rev. B **64**, 125411 (2001).
[26]H.-N. Yang, Y.-P. Zhao, G.-C. Wang, and T.-M. Lu, Phys. Rev. Lett. **76**, 3774 (1996).
[27]A. Palmero, N. Tomozeiu, A. M. Vredenberg, W. M. Arnoldbik, and F. H. P. M. Habraken, Surf. Coat. Technol. **177–178**, 215 (2004).
[28]A. Palmero, H. Rudolph, and F. H. P. M. Habraken, J. Appl. Phys. **101**, 083307 (2007).
[29]A. Borrás, A. Yanguas-Gil, A. Barranco, J. Cotrino, and A. R. González-Elipe, Phys. Rev. B **76**, 235303 (2007).
[30]M. Zhang, G. Lin, C. Dong, and L. Wen, Surf. Coat. Technol. **201**, 7252 (2007).
[31]M. Moseler, P. Gumbsch, C. Casiraghi, A. C. Ferrari, and J. Robertson, Science **309**, 1545 (2005).